RISET
Geologi dan Pertambangan
Indonesian Journal of Geology and Mining
https://jrisetgeotam.lipi.go.id
LIPI

Research article

Geothermal Reservoir Identification based on Gravity Data Analysis in Rajabasa Area-Lampung

Riset Geologi dan Pertambangan
Indonesian Journal of Geology and Mining
Vol.31, No 2, pages 77–97

doi:
10.14203/risetgeotam2021.v31.1164

Keywords:
Geothermal,
Gravity,
Lampung,
Rajabasa,
Reservoir.

Corresponding author:
Rahmat Catur Wibowo
E-mail address:
rahmat.caturwibowo@eng.unila.ac.id

Article history
Received: 26 February 2021
Revised: 6 September 2021
Accepted: 22 September 2021

Muh Sarkowi[1], Rahmat Catur Wibowo[1]
[1]Department of Geophysical Engineering, Faculty of Engineering, Lampung University

ABSTRACT Gravity research in the Rajabasa geothermal prospect area was conducted to determine geothermal reservoirs and faults as reservoir boundaries. The research includes spectrum analysis and separation of the Bouguer anomaly to obtain a residual Bouguer anomaly, gradient analysis using the second vertical derivative (SVD) technique to identify fault structures or lithological contact, and 3D inversion modeling of the residual Bouguer anomaly to obtain a 3D density distribution subsurface model. Analysis was performed based on all results with supplementary data from geology, geochemistry, micro-earthquake (MEQ) epicenter distribution map, and magnetotelluric (MT) inversion profiles. The study found 3 (three) geothermal reservoirs in Mount Balirang, west of Mount Rajabasa, and south of Pangkul Hot Spring, with a depth of around 1,000-1,500 m from the ground level. Fault structures and lithologies separate the three reservoirs. The location of the reservoir in the Balirang mountain area corresponds to the model data from MEQ, temperature, and magnetotelluric resistivity data. The heat source of the geothermal system is under Mount Rajabasa, which is indicated by the presence of high-density values (might be frozen residual magma), high-temperature values, and the high number of micro-earthquakes epicenters below the peak of Mount Rajabasa.

INTRODUCTION

Geothermal potential in Mount Rajabasa - Kalianda Lampung is indicated by the presence of geothermal manifestations around Mount Rajabasa. Geothermal manifestations are found at the south and north of Mount Rajabasa: Kumbang Sumur, Kecapi, and Rajabasa hot springs, Kunjir fumarole and mud pools, and the geysers of Mount Botak. Mount Rajabasa has two peaks (Mount Balirang and Rajabasa), and four craters (peak of M. Rajabasa, peak of M. Balirang, Way Sulerang at Sukamandi Village, and Simpur) (Mussofan et al., 2015) (Figure 1).

The north-south trending structure caused by tectonic influences (Sumatra Fault Zone) controls the permeability in the Rajabasa geothermal system. The structure extends to the top of Rajabasa and Balirang. Therefore, it is essential to study the development of the structure in this area that related to the Rajabasa geothermal system.

Rasimeng (2008) conducted a magnetic study to identify the presence of faults in the Rajabasa geothermal area. The results obtained were only able to identify a significant fault with a southeast-northwest direction. Identification of faults using Radon and Thoron indicated two faults in the southeast. However, the results are not compatible to the regional geological map of the area (Haerudin et al., 2013). Fault identification and fluid flow using gravity and audio- magnetotelluric (AMT) methods show the presence of 2 normal faults in the south with a southeast-northwest direction (Haerudin et al., 2014). Daruwati (2014) analyzed the presence of faults based on magnetic anomaly analysis, and found two faults trending southeast - west in the west. Fault identification has also been carried out based on LIDAR data analysis that found the main structure of the fault trending southeast-northwest (Mussofan et al., 2015). Previous researches on faults identification were regional and concentrated in the southeast. For this reason, further research is needed, especially to identify the details of the fault structure in the Rajabasa geothermal prospect area. These faults control the reservoir in the geothermal system of Mount Rajabasa.

The existence of geothermal reservoir locations is one of the main targets in conducting exploration either by using geological, geochemical, and geophysical studies. Based on the results of the Magnetotelluric (MT) study, the geothermal reservoir of the Rajabasa geothermal prospect area is in the Pangkul and Cagung areas (Saefulhak, 2017). Mussofan et al. (2016) conducted a study of MT, geology, and geochemistry, and found the existence of a geothermal reservoir in the Balirang mountain area, which is an up-flow zone. Efforts to identify geothermal reservoirs have been carried out using the 1D sounding resistivity method, and found a reservoir at a depth of 450 m, which might be sandy tuff rock. However, the electrode spacing is too short (AB/2 = 600 m). This sounding will only detect subsurface structures at a depth of less than 300 m.

The geothermal reservoir of Mount Rajabasa Kalianda has a moderate temperature reservoir of 212.08°C (Haerudin et al., 2009). Geological and geochemical analysis in the study area provide reservoir temperatures for each manifestation: 240 – 260°C in Way Merak, 270 – 300°C in Cugung, and 260 – 280°C in Pangkul manifestation. The up-flow zone is estimated to be between Pangkul or Cugung, which has a relatively high value of non-condensable gasses (NCG) and CO_2. Farther south, it is closer to the outflow zone (Mussofan et al., 2016). Nevertheless, more detailed research is necessary to determine the location of the Rajabasa geothermal reservoir. Detailed mapping and its relation to the presence of any fault structures or lithology is required, because faults or any lithological boundaries might control the existence of a reservoir. This research was conducted by processing gravity data, including spectrum analysis, gradient analysis, and 3D inversion modeling. The results are then compared and correlated with geological, geophysical, and geochemical data from previous published researches.

GEOLOGY RAJABASA

Mount Rajabasa is a young volcanic unit composed of andesite-basalt lava, breccia, and tuff (Mangga et al., 1993), with Lampung Formation and Tertiary andesite around. The volcanic activity of Mount Rajabasa began with the formation of a pre-Rajabasa volcanic cone, which then followed a large

eruption that formed the pre-Rajabasa Caldera (Saefulhak, 2017). Pre-Rajabasa Mountains, Rajabasa Mountains, and Balirang Mountains in the pre-Rajabasa caldera are formed in depression areas that form cone-shaped volcanoes, forming rocks in the form of basaltic-andesitic lava, volcanic breccias, and tuff (Figure 1) (Hasibuan et al., 2020).

Regional stratigraphy is closely related to the Rajabasa pre-caldera. The Quaternary Mount Rajabasa Complex with Mount Rajabasa and Mount Balirang are the main eruption centers interpreted as post-caldera volcanism. Volcanic products associated with the Quarter age caldera include Tertiary andesite (Tpv), which is exposed at the southeastern tip of the caldera. The older andesite units are composed of andesitic lava as a product of Tertiary volcanism spreading from the west to the

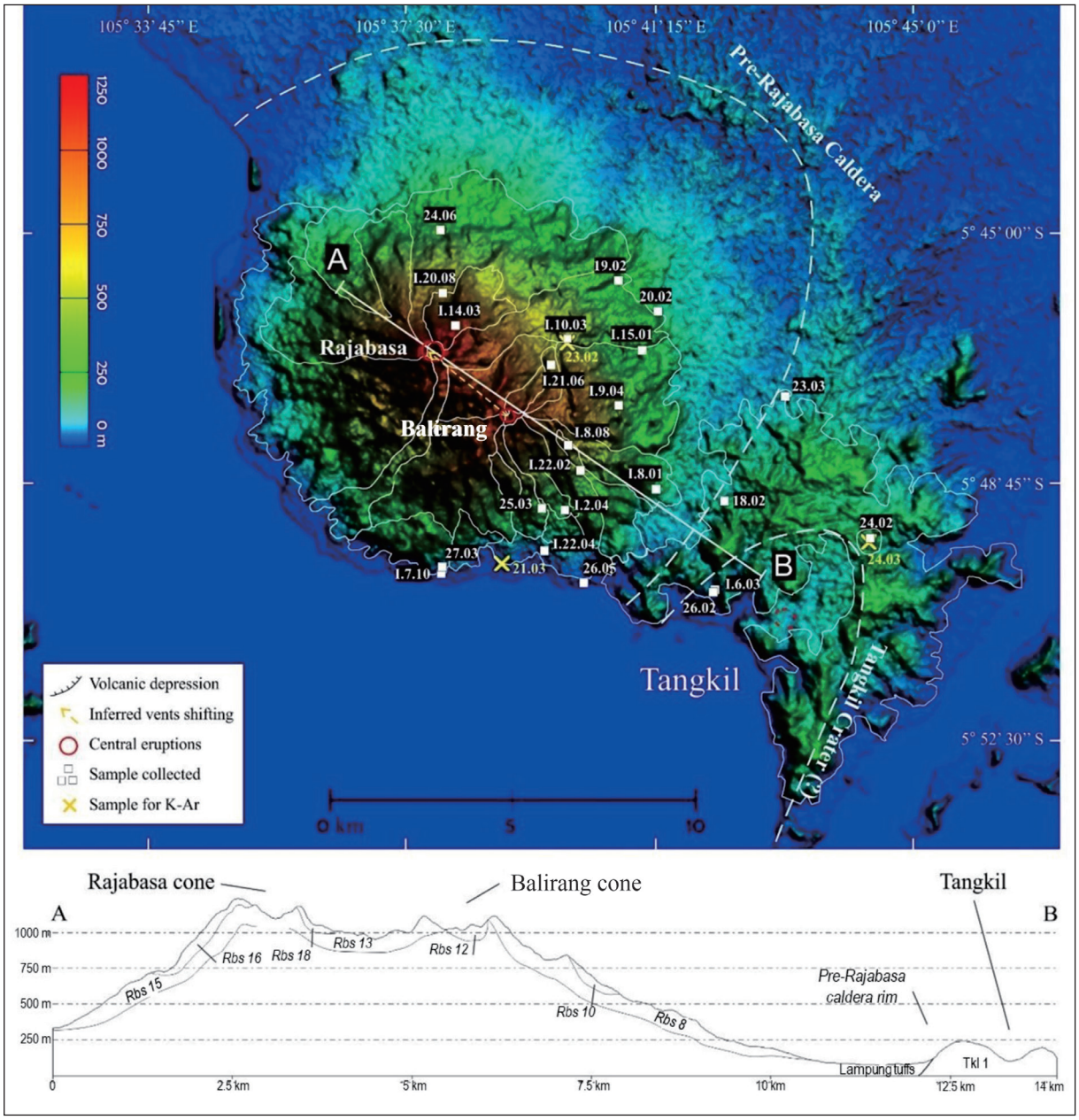

Figure 1. ASTER image showing Mount Rajabasa and Mount Balirang located in the pre-Rajabasa caldera, as well as a topographic cross section with a NW-SE direction (Hasibuan et al., 2020).

southeast of Mount Rajabasa. Based on the characteristics of the lava flows that occur on Mount Rajabasa, andesite units are estimated to develop not far from the eruption source (Bronto et al., 2012).

The volcanic products of the Rajabasa complex can be divided into five periods (Suswati et al., 2001), from old to young (Figure 2):

1. The Tua Tangkil Volcanic Product consists of the Pliocene-aged Pliocene Volcanic Product Unit (Tv)
2. Pematang Taman Old Volcanic Products consists of Pleistocene Old Volcanic Product Unit of Pematang Taman (PTv).
3. The product of the Balirang Volcano consists of the Balirang Flow Pyroclastic Unit (Bl) and the Balirang Lava Unit (Ba), which are of the Pleistocene age.
4. Hillside Eruption Product 845 consists of Lava Unit 845 (8451), which is Pleistocene in age.
5. The product of the Rajabasa Volcano consists of the Rajabasa Flow Pyroclastic Unit (Ra) and the Rajabasa Lava Unit (Rl), which are Pleistocene in age.

The fault that controls geothermal in the Mount Rajabasa complex is the Lampung Fault with a northwest-southeast direction. The Lampung Fault is a shear fault that controls the geothermal system in the north and southeast of Mount Rajabasa. Local faults are normal faults and control the geothermal system in the southern part. The fault structure in the Rajabasa mountain area has a northwest-southeast trending structural configuration parallel to the Sumatran fault. These faults are young faults that control the boundaries of resource reserves, fluid paths, and the potential for resource compartmentalization in shallow sections (Rajabasa shear fault and Simpur normal fault). Meanwhile, the southwest-northeast faults (Balirang normal fault and Botak normal fault) are older and control the basement configuration so that it affects the thickness of the reservoir (Figure 2) (Suswati et al., 2001; Rasimeng, 2008; Daruwati, 2014).

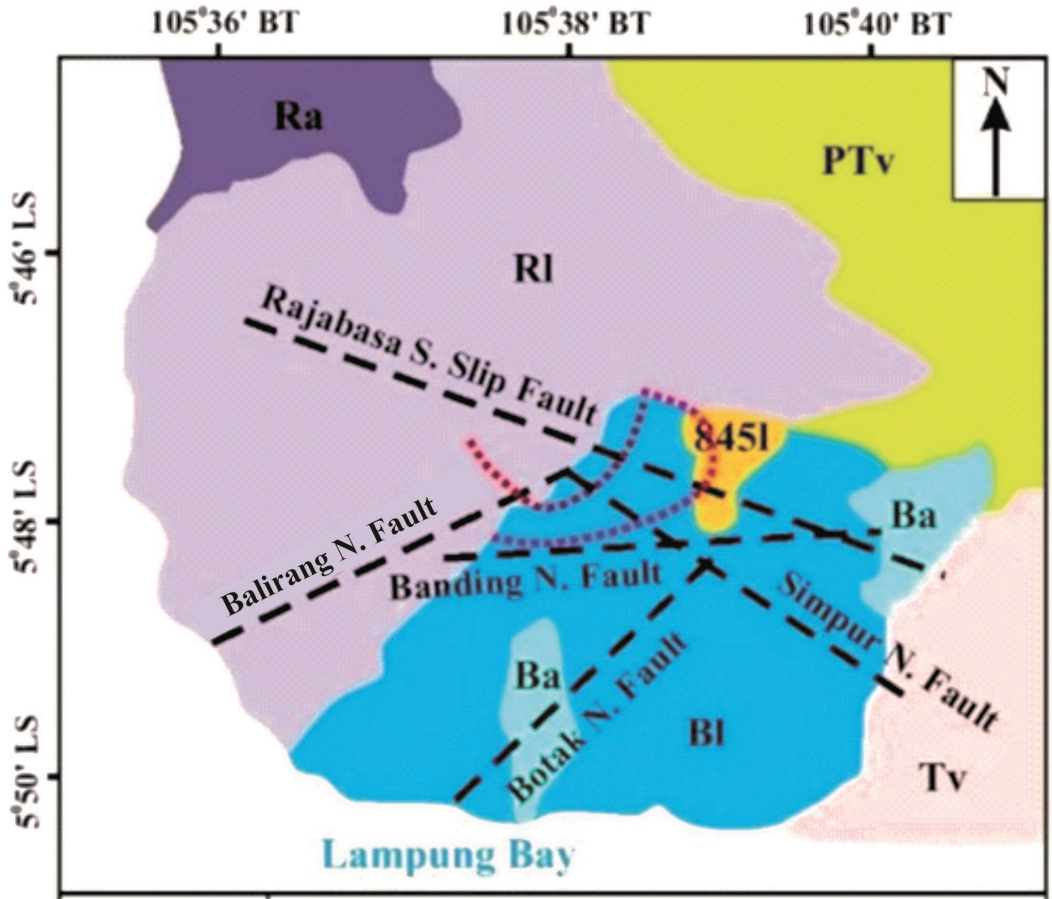

Age		System	Map Unit	Lithology
Quarternary	Pleistocene	Rajabasa	Rl Rajabasa Lava	Andesite lava to basaltic andesite
			Ra Rajabasa Pyroclastic Flow	Pyroclastic shaped as block flow and ash deposit
		Bukit 845	8451 Lava 845	Basaltic andesite lava
		Balirang	Bl Lava Balirang	Basaltic andesite lava, basaltic andesite, and andesite
			Ba Balirang Pyroclastic Flow	Pyroclastic shaped as ash flow deposit
		Pematang Taman	PTv Ancient volcanic product Pematang Taman	Basaltic andesite lava with pyroclastic shaped as block flow and volcanic ash
Tertiary	Pliocene	Tangkil	Tv Ancient volcanic product Tangkil	Andesite fragmented embedded in base mass coarse sand

Figure 2. Pre-Rajabasa Caldera based on the results of DEM interpretation (Suswati et al., 2001).

The gravity data used in this study is secondary data from measurements carried out by the Bandung Geological Survey Center in 1991. The gravity data used were from 272 stations, consisting of 16 measurement trajectories scattered around Mount Rajabasa from bottom to top (Buyung and Walker, 1991). The gravity data was corrected to obtain the Bouguer anomaly. We applied spectrum analysis on several paths to obtaining the depth limit of the regional and residual Bouguer anomalies. Therefore, the width of the windows used to perform the Bouguer anomaly filter could be determined. The power spectrum of the Bouguer anomaly is carried out by performing a Fourier transformation of the gravity data into the frequency domain (Blakely, 1995):

$$F(g) = 2\pi\gamma m \frac{e^{|k|(z_0 - z_1)}}{|k|} \quad (1)$$

The energy spectrum of the equation is:

$$E(k) = \frac{4\pi^2\gamma^2\rho^2}{|k|^2} e^{-2|k|z} \quad (2)$$

$$\log E(k) = \log(4\pi^2\gamma^2\rho^2) - 2|k|z - 2\log|k| \quad (3)$$

$$\log E(k) = \log A - 2|k|z \quad (4)$$

with z_0 is the depth of measurement point, z_1 is the depth of the center of mass, $z_1 > z_0$, $k = 2\pi/\lambda$ (wave number), λ is wavelength, g is gravity anomaly, ρ is density. The wavelength and depth of the anomalous object can be determined based on that equation.

The moving average filter was used to separate regional and residual Bouguer anomalies (Abdelrahman, 1996). The calculation of the moving average is done by averaging the anomaly values for several points of gravity, as shown by the equation (Setiadi et al., 2010):

$$\Delta g_{Reg}(i,j) = \frac{(\Delta g(i-n, j-n) + \ldots + \Delta g(i,j) + \ldots + \Delta g(i+n, j+n))}{N}$$

with $n = \frac{N-1}{2}$, and N must be odd numbers.

The result of this averaging is the regional anomaly. In contrast, the residual anomaly is obtained by subtracting the data from the gravity measurement with the regional anomaly.

Second vertical derivative (SVD) analysis of the Bouguer anomaly was carried out to obtain fault structures/intrusions/lithological boundaries and sources of anomalies originating close to the surface (Elkins, 1951; Blakely, 1995). For gravity data in a regular grid, the SVD anomaly can be derived through a filtering process by convoluting the gravity anomaly with the SVD filter (Elkins, 1951):

$$\Delta g_{svd}(\Delta x, \Delta y) = \int_{-\infty}^{\infty}\int_{-\infty}^{\infty} \Delta g(x,y) F(x - \Delta x, v - \Delta y) dx dy$$

with F is SVD filter and Δg is gravity anomaly as input data.

The SVD value of the Bouguer anomaly of zero (0) indicates a reasonably significant density change in the form of faults, anomalous object boundaries, lithological boundaries, and basin boundaries (Sumintadireja et al., 2018).

Bouguer anomaly 3D inversion modeling was prepared using GRAV3D 2.0 program (Jones, 2006) to obtain a subsurface density distribution model (Witter et al., 2016; Sarkowi and Wibowo, 2021).

Then, we correlated the resulted density distribution model with geological, geochemical, and other geophysical data. The outcome is the fault structure model, reservoir, and heat source of the geothermal system of Mount Rajabasa. The correlation between the fault structure/lithological boundary with the prospect of a geothermal reservoir area, which is obtained from gravity inversion modeling, geological, geochemical data, magnetotelluric model, and MEQ maps, can be used to determine the presence of compartments of the geothermal system in the Rajabasa geothermal prospect area (Harvey, 2014).

RESULT AND DISCUSSION

Bouguer anomaly map is correlated with geothermal manifestation data, the presence of volcanoes and craters in the geothermal prospect area of Mount Rajabasa, as shown in Figure 3. The study area has a high Bouguer anomaly (80 mGal) in the north and southeast, while the middle and southwest have low anomalies (28 mGal) with anomalous patterns extending from east to west. The area between Mount Rajabasa - Balirang has the lowest anomaly (Figure 3).

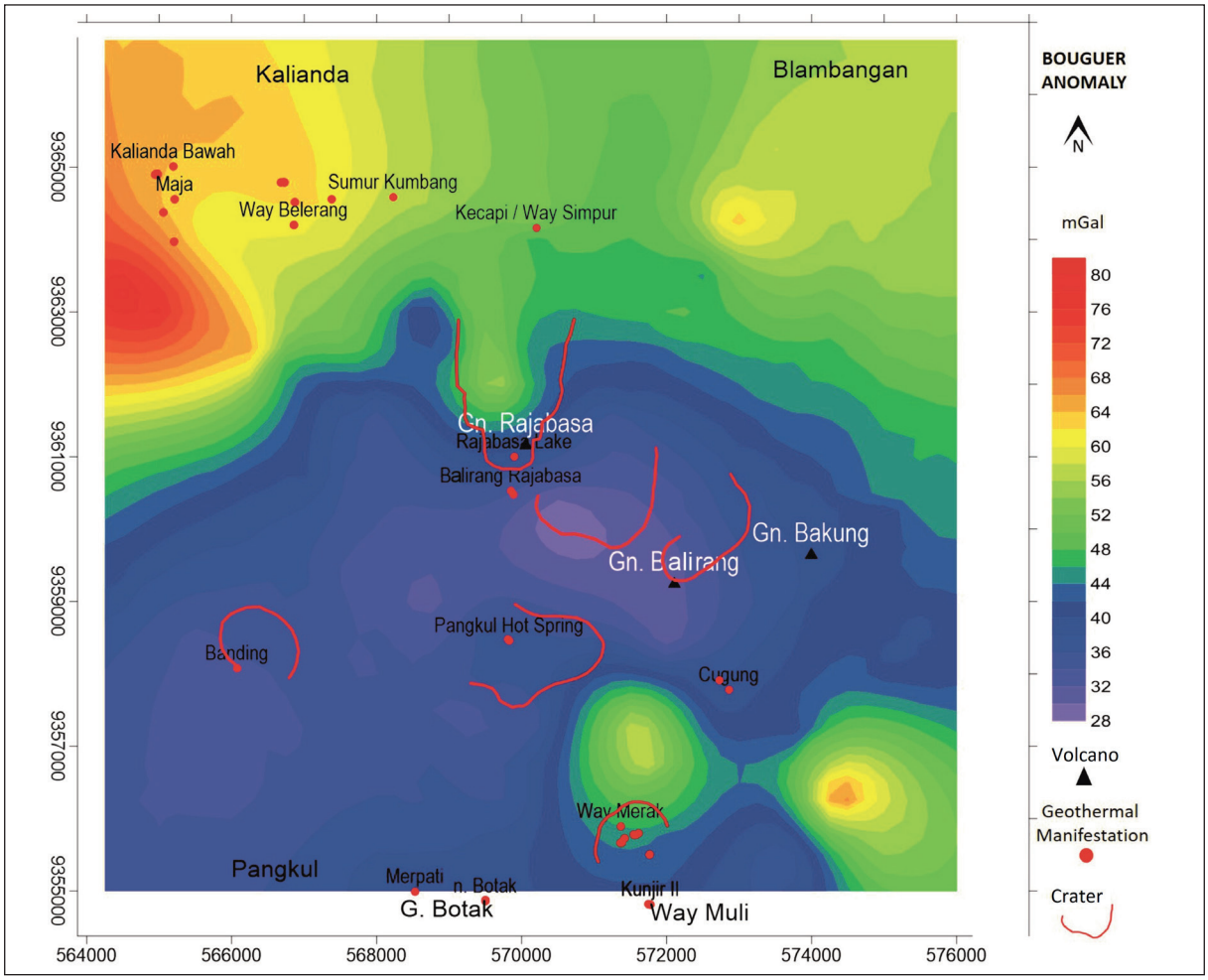

Figure 3. Bouguer anomaly geothermal prospect area in Rajabasa area.

Bouguer anomaly is the total anomalies originating from several sources of anomalous objects: deep (regional), shallow (residual), and noise (Blakely, 1995). We applied spectrum analysis to find the depth of these anomaly sources. The spectrum analysis results from the four lines of Bouguer anomalies indicate the depth limit of the regional and residual anomaly of 4,250 m (Figures 4a and 4b).

Based on the spectrum analysis results, we filtered the Bouguer anomaly using the moving average method with 8,500 m windows to obtain the residual Bouguer anomaly (Abdelrahman, 1996). Figure 5 shows the Bouguer Residual Anomaly, which overlays geothermal manifestations, volcanoes, and craters in the Rajabasa geothermal prospect area.

The residual Bouguer anomaly has a value from -9 mGal to 20 mGal with a high anomaly (positive) located in the Way Merak area, the peak of Mount Rajabasa, the northern area (Way Balirang, Kumbang, and Kecapi wells), and a little in the west. The low residual Bouguer anomaly is found in, south of Mount Rajabasa, south of Pangkul hot spring, and the manifestation area of Lower Kalianda.

The high anomaly around Mount Rajabasa (15 mGal) indicates that residual magma flows under the crater of Mount Rajabasa. In contrast, the high anomaly at the other locations might be related to the remnants of mountain formation in the pre-Rajabasa period. The low anomalies in Mount Balirang, west of Mount Rajabasa, and the area of Pangkul hot spring are probably geothermal reservoir prospects. To determine the boundaries of the prospect of a geothermal reservoir, we need more supporting data, such as geological (fault structures), geochemistry, and other geophysical data (Harvey, 2014).

An SVD analysis of the residual Bouguer anomaly was performed to obtain the pattern of fault structures and lithological boundaries from the gravity data. An SVD value of zero (0) indicates a significant change in density in the form of faults, anomalous object boundaries, lithological boundaries, and basin boundaries (Sumintadireja et al., 2018). Figure 6 shows an SVD map of the residual Bouguer anomaly calculated using the Elkins filter (Elkins, 1951). The residual Bouguer anomaly SVD map shows the main fault pattern in north-south, west-east direction, and a secondary fault with an northwest-southeast direction.

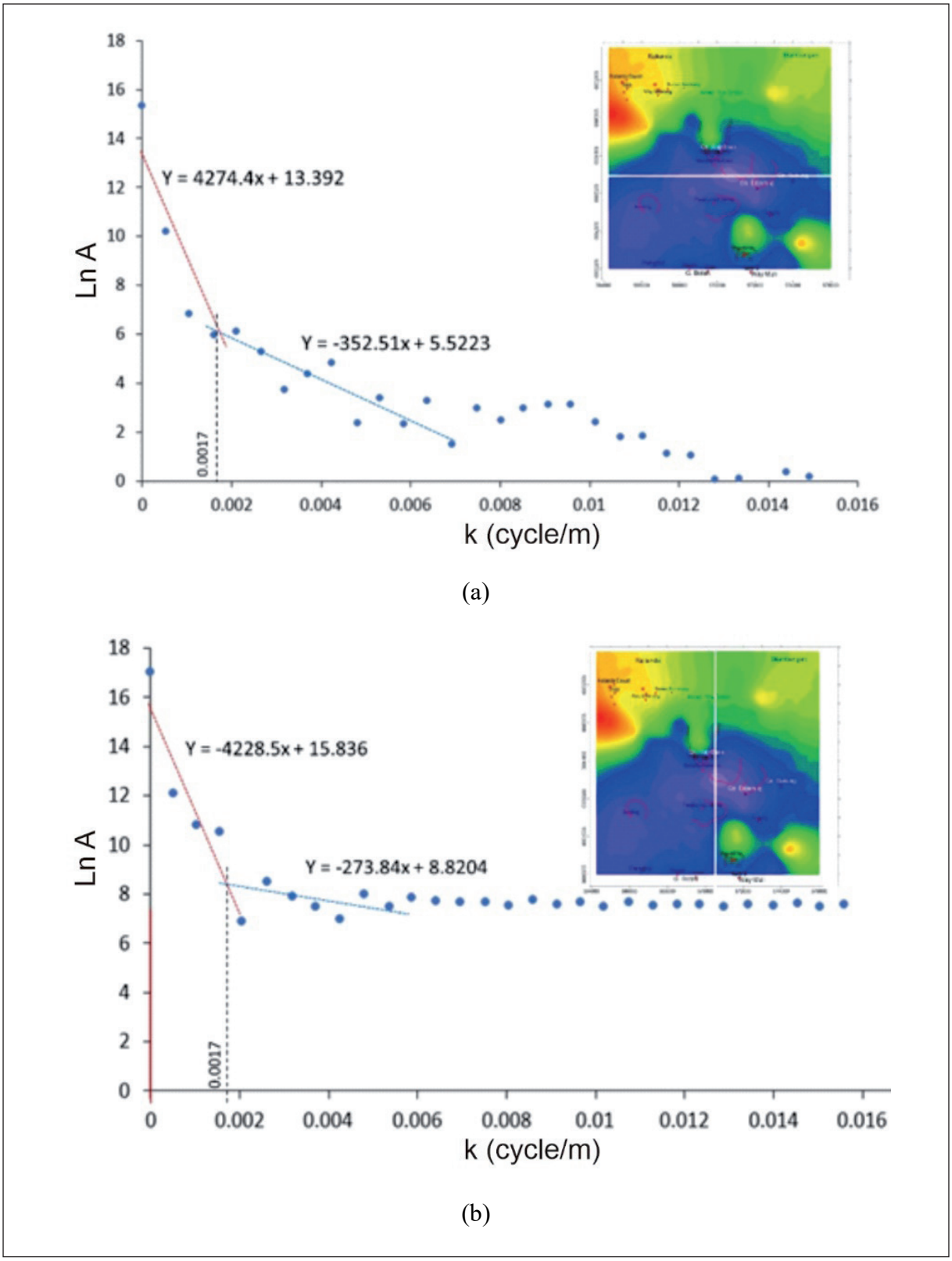

Figure 4. (a) Spectrum analysis of the west – east trajectory which has a regional anomaly boundary and a residual of 4,274 m, and (b) A north – south trajectory which has a regional anomaly boundary and a residual of 4,228 m.

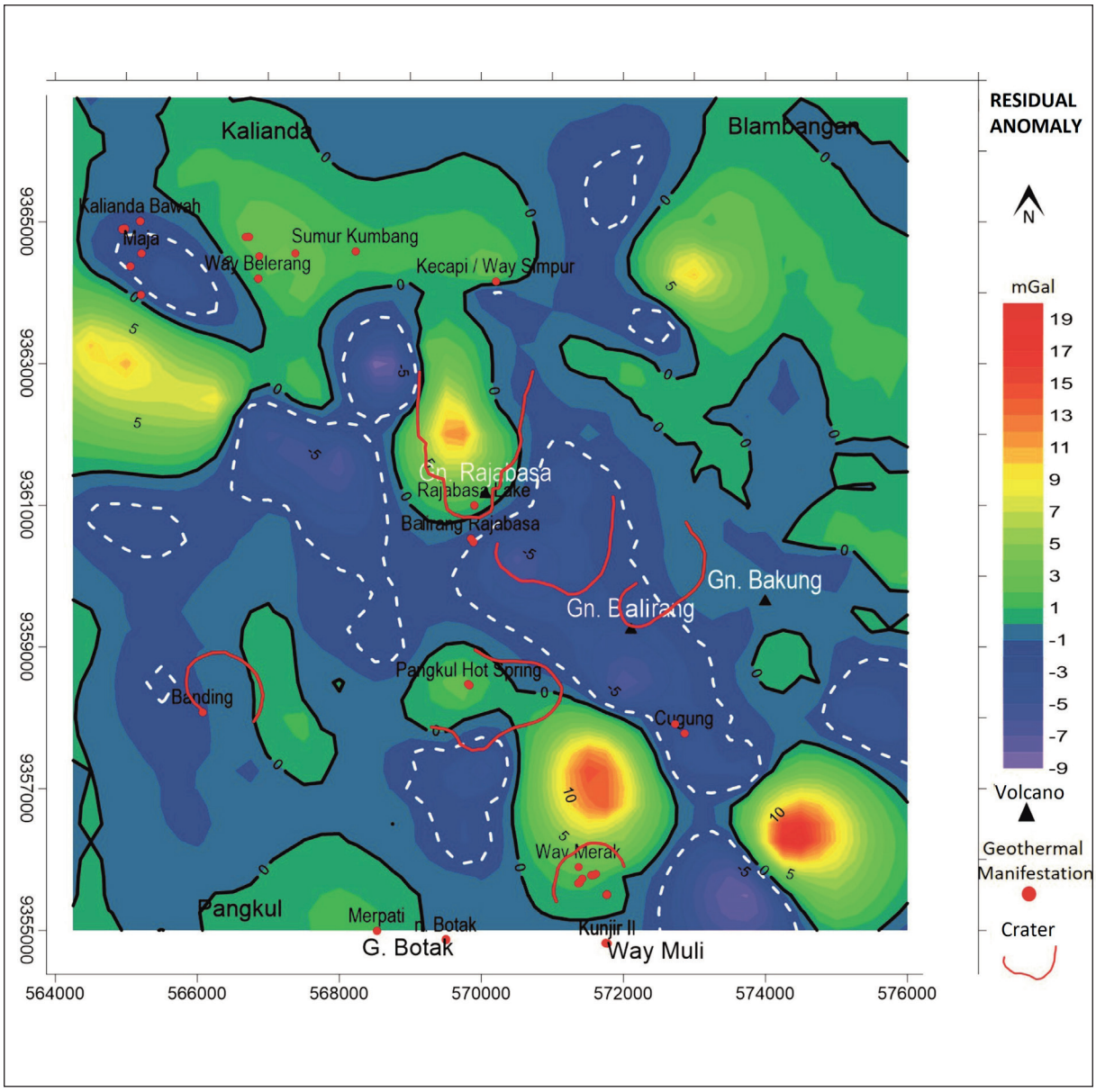

Figure 5. Map of residual Bouguer anomaly with data of geothermal manifestations, volcanoes, and craters in the prospect area.

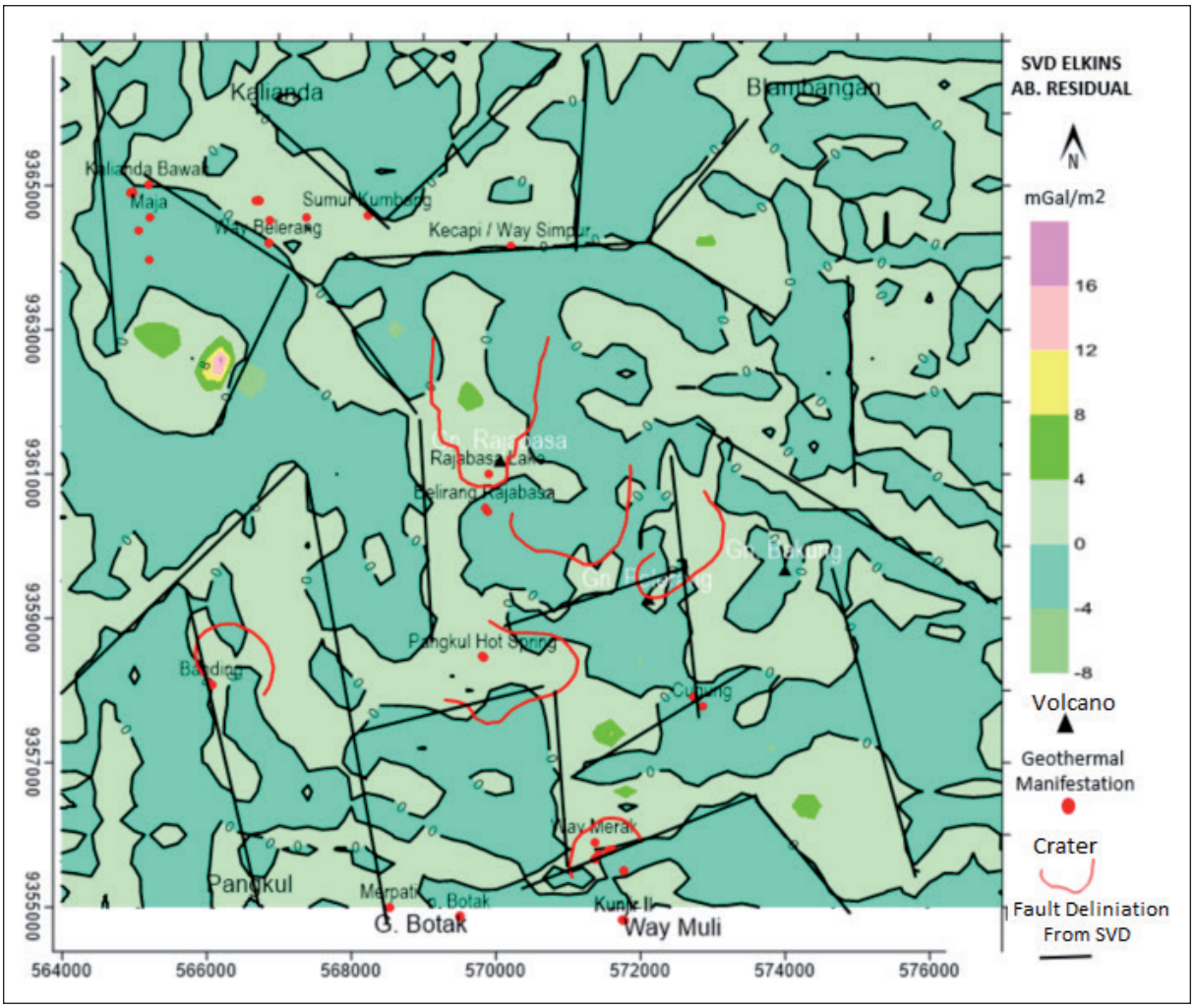

Figure 6. Map of SVD anomaly from filtering the residual Bouguer anomaly with Elkins filter (Elkins, 1951) and the interpretation of the presence of faults (black lines).

The existence and location of faults in geothermal areas is a fundamental aspect because they might transmit or bound the fluid movement, which would control the existence of geothermal reservoirs (Brehme et al., 2016). Analyzing the compilation of the low residual Bouguer (<0 mGal), fault structure from SVD analysis, temperature data, the MT and MEQ model, we can analyze qualitatively and quantitatively the geothermal reservoir in the area (Figure 7).

The patterns from the residual Bouguer anomaly map show three reservoir prospect areas separated by the presence of a fault structure derived from the SVD analysis. The existence of these three reservoirs is correlated with the ones derived from MEQ and MT anomalies. The temperature data indicate that the reservoirs are in a high-temperature region.

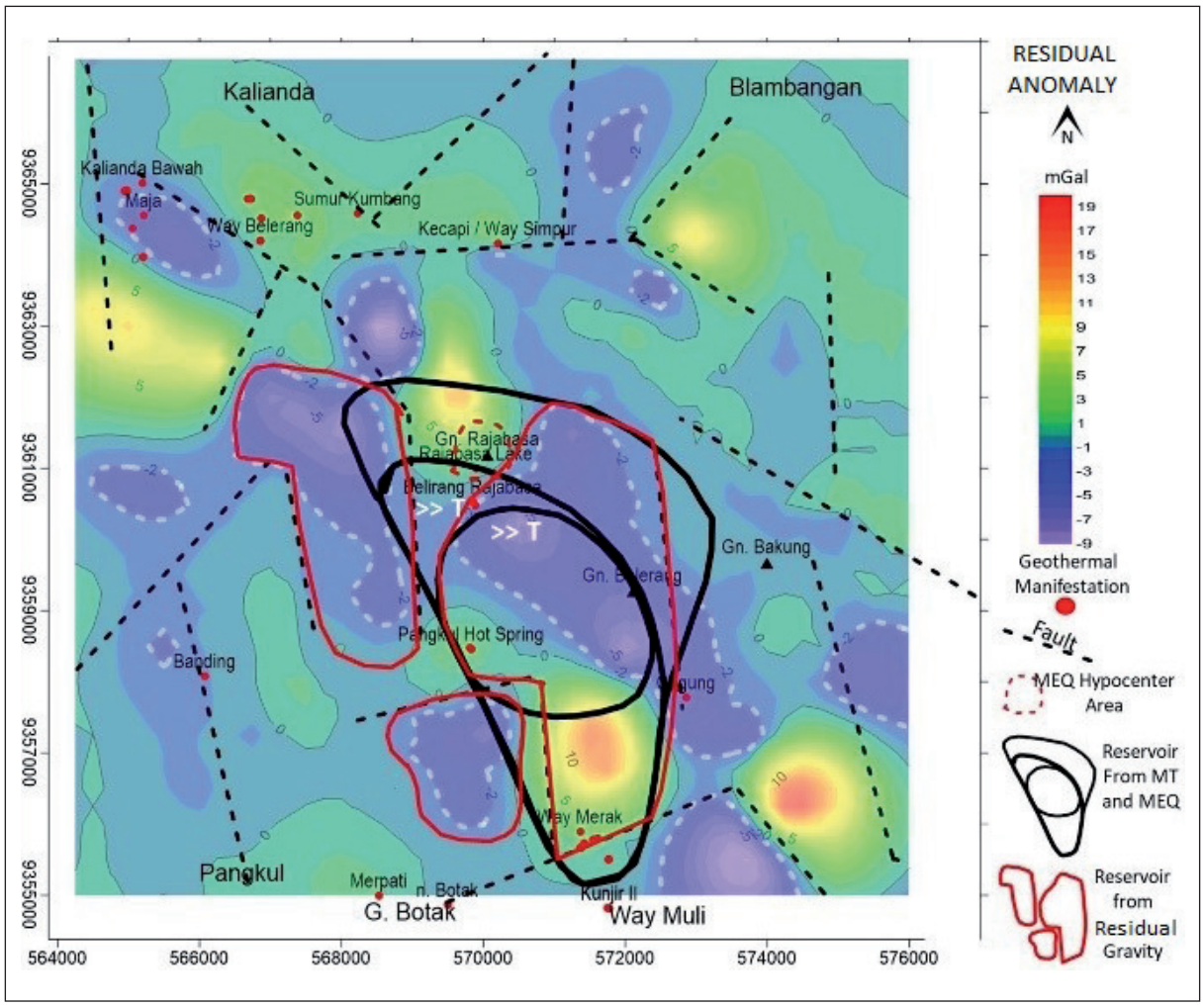

Figure 7. Compilation map of residual Bouguer anomaly, fault structure, temperature data, MT and MEQ data on the Rajabasa geothermal prospect.

A good reservoir will generally have high porosity, permeability, and relatively low density compared to its surroundings (Björbsson and Bodvarsson, 1990). A quantitative interpretation was carried out in 3D inversion modeling of the residual Bouguer anomaly using the GRAV3D program (Jones, 2006) to obtain a subsurface density model in this study. The subsurface density distribution model resulting from the inversion modeling of the residual Bouguer anomaly is shown in Figure 8.

Rajabasa Geochemistry

Geothermal manifestations in Mount Rajabasa are scattered in the northern, central, and southern region (Figure 9). The northern geothermal manifestations have lower temperatures than those in the central and southern parts. High manifestation temperatures are in Way Merak (101°C), Mount Botak (100°C), Pangkul (96°C), and Cugung (96°C). The pH value of the northern manifestation is higher than of the southern manifestation (Mussofan et al., 2015).

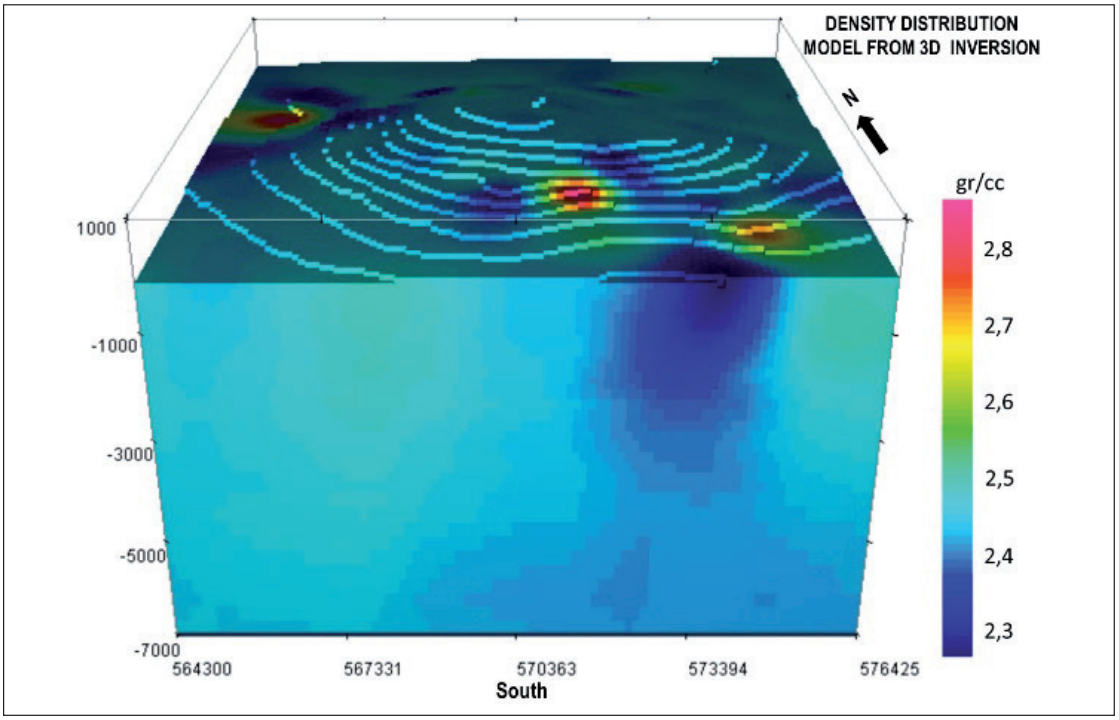

Figure 8. Subsurface density distribution model results from 3D inversion modeling of residual Bouguer anomaly.

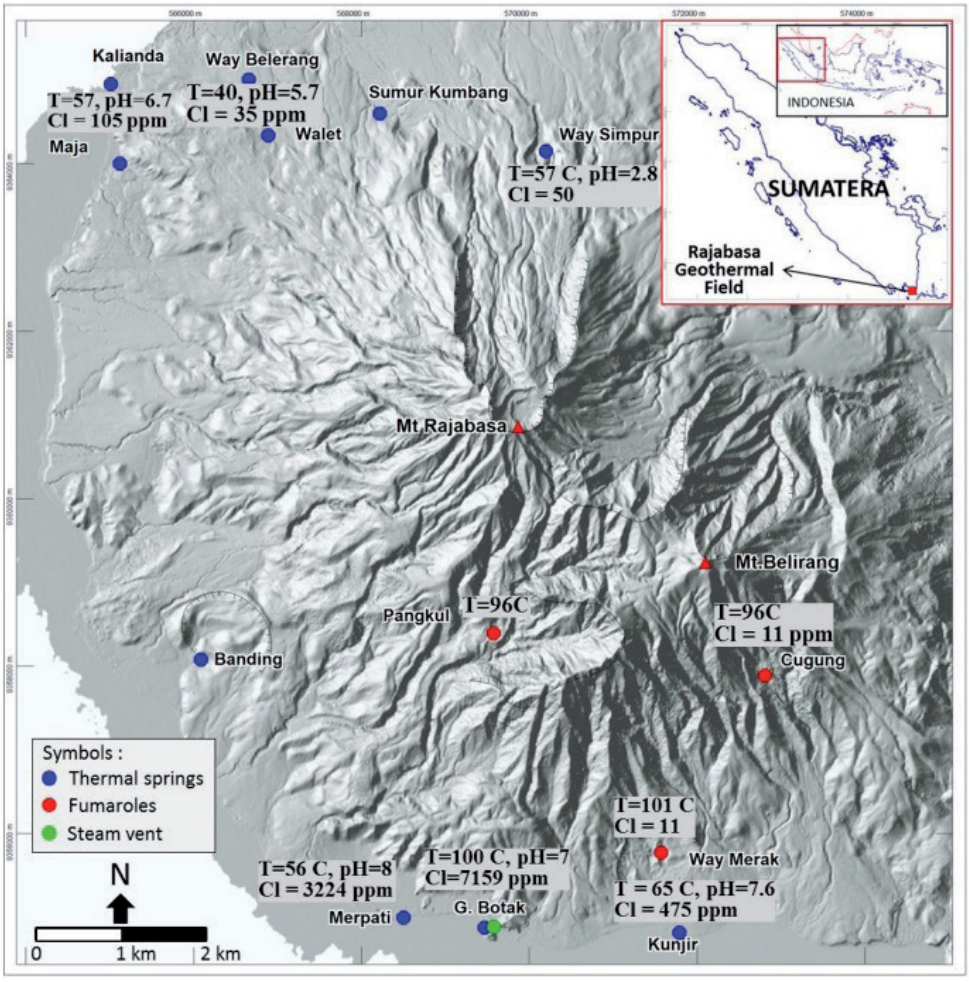

Figure 9. Location of manifestations in the Rajabasa geothermal field (Mussofan et al., 2015).

The manifestation on the northern slope consists of sulfate and bicarbonate hot springs, while the manifestation on the southern slope consists of fumaroles, sulfate, and chloride hot springs. Most of the chloride hot springs have seawater as the source, except the Mount Botak springs, which is a mixture of sea water and reservoir water. The upflow area might be located between Pangkul (240-270°C), Cugung (240-300°C), and kaipohan (nonthermal manifestation) fumaroles, with outflow towards Way Merak (220-240°C). Analysis result and heat distribution map indicate the high heat distribution between Mount Rajabasa – Balirang and Pangkul (Saefulhak, 2017).

The Cl-SO_4-HCO_3 diagram shows that most liquid samples from the manifestation in the northern area are steam-heated water, and the rest are peripheral water (Saefulhak, 2017). The N_2-CO_2-Ar ternary plot shows that the trend of CO_2/N samples from Pangkul, Cugung, and Way Merak may be a unitary geothermal system (Saefulhak, 2017). HAr-CAr gas shows the geothermometer values for samples from Way Merak ranging from 260-265ºC. HSH-FT gas shows the geothermometer value for samples from Way Merak is 300-325ºC. Most samples were from Way Merak, which indicate ^{18}O enrichment. The similarity of the isotopic composition between Way Balirang in the north and Way Merak in the south indicates the possibility of similarity in the recharge area and the direction of its recharge (Saefulhak, 2017).

Magnetotelluric (MT)

The west-east MT inversion model in Figure 10 indicates a thick and deep low-resistivity layer (conductive layer) at the west. At the middle part between Pangkul and Cugung manifestation, there is a relatively thin and shallow low-resistivity layer, and thickened to the west. The eastern boundary is indicated by the disappearance of the low-resistivity layer (Saefulhak, 2017).

Resistivity model from MT inversion in NNW – SSE path (Figure 11) indicates a low resistivity layer (conductive layer) that continues from the north (Way Simpur) towards the peak and down towards Pangkul and Way Merak. The low resistivity layer (the conductive layer between the Rajabasa – Pangkul peaks is relatively flat (Figure 11) (Saefulhak, 2017).

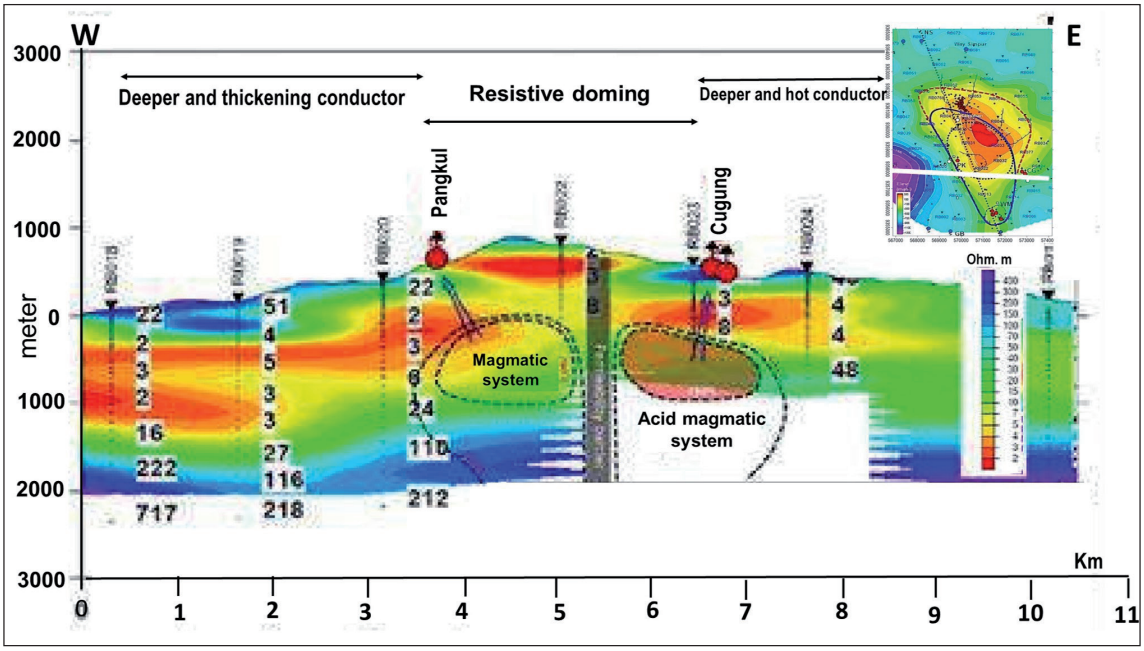

Figure 10. The resistivity distribution model from the 1D MT inversion modeling for the west – east profile (Saefulhak, 2017).

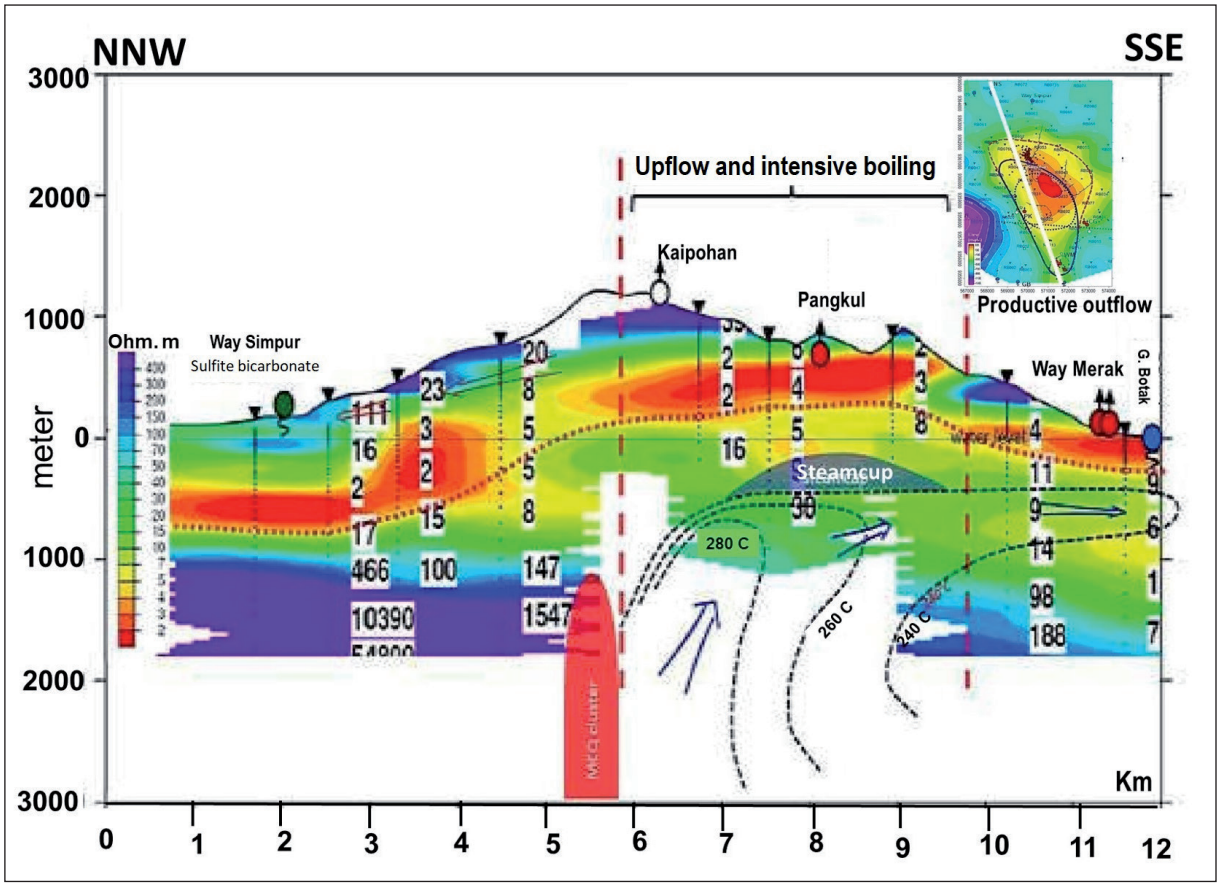

Figure 11. The resistivity distribution model from the MT 1D inversion modeling for NNW – SSE profile (Saefulhak, 2017).

The two MT inversion resistivity models show a relatively similar trend. A distinct low resistivity (conductive) layer structure underneath the peak, which is common in geothermal systems. The low resistivity or conductive layer extends beyond the northern manifestation area. Below the Rajabasa peak at a depth of 1,000 m from the mean sea level (MSL), the conductive layer disappears. It can be interpreted that the young volcanic core or the central volcanic facies below the summit, which is commonly associated with many intrusion, lava plugs, and breccias, are too impermeable for hydrothermal circulation to pass. So it is assumed that the area below the Rajabasa peak acts as a permeability boundary that divides the geothermal system into two parts: north and south (Saefulhak, 2017).

Microearthquake (MEQ)

The microearthquake (MEQ) survey in the Rajabasa area found that micro-earthquake epicenters are concentrated under Mount Rajabasa, spreading to the northwest-southeast. The distribution of the epicenters might be related to volcanic activity under Mount Rajabasa. Inversion modeling of shear wave splitting and polarization-time delay provide the fracture orientations, which mostly have the north-south direction (Figure 12) (Saefulhak, 2017).

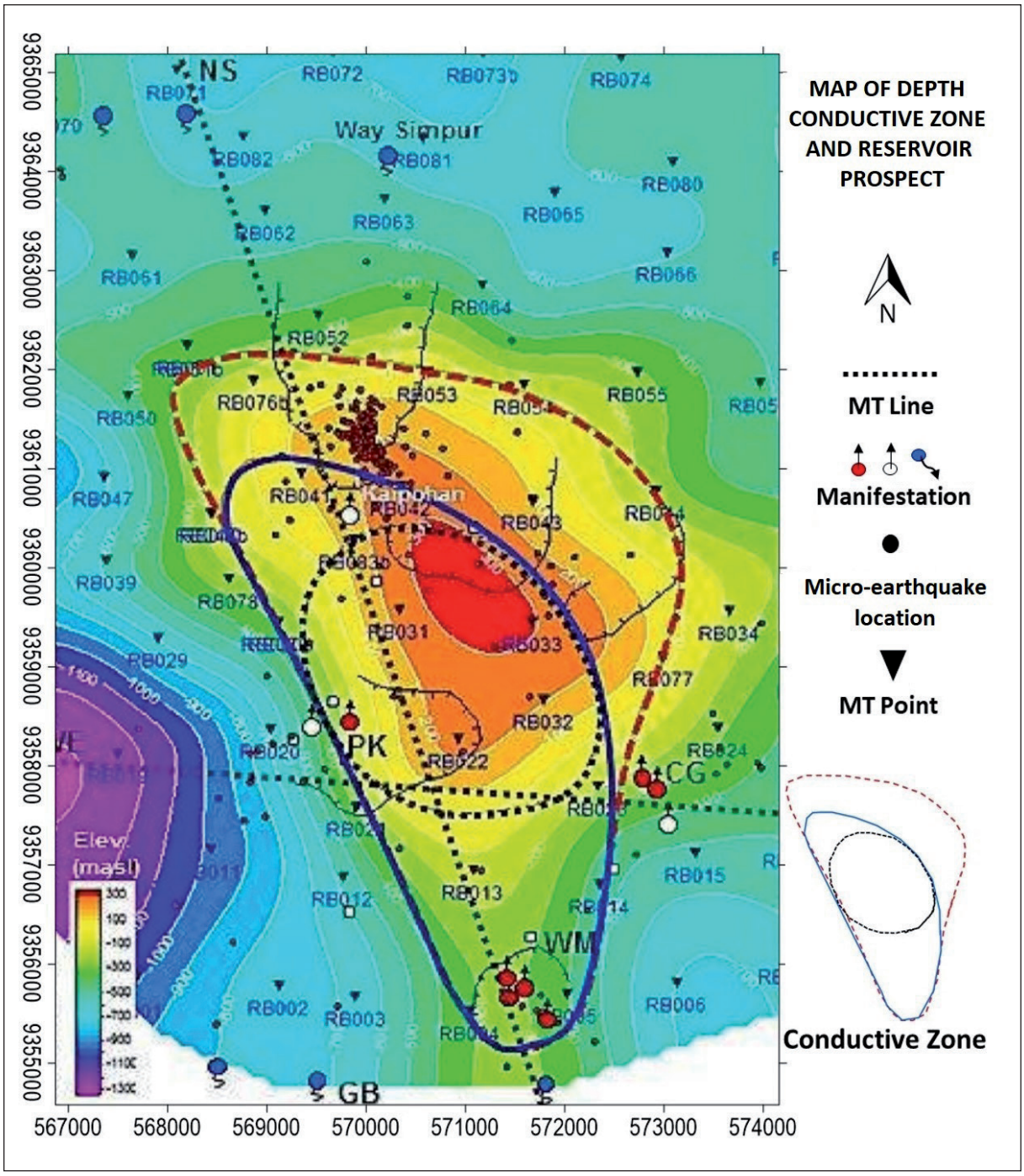

Figure 12. Conductive zone elevation map based on the MT inversion modeling and MEQ interpretation (Saefulhak, 2017).

In Figure 12, the red dotted line shows the boundaries of the conductive zone (including at the top of Mount Rajabasa and its north), which is interpreted as the outer boundary of the Rajabasa geothermal reservoir prospect derived from MT data. The existence of a reservoir under the peak of Mount Rajabasa is also supported by MEQ data, which shows the number of micro-earthquakes under Mount Rajabasa. The blue line is the geothermal reservoir prospect area that does not include the peak of Mount Rajabasa. Meanwhile, the area bounded by a dotted line shows the prospect of a reservoir that does not include the peak area and the southern part (Saefulhak, 2017).

Reservoir constraints

Figure 13 shows the low-density distribution model compiled with geological data (manifestations, volcanoes, craters), geothermal reservoir prospect data from MEQ, MT, and temperature data. The compilation indicates that the low-density areas correlate with reservoir prospects derived from MEQ, MT, and temperature data. Areas with low-density distribution (<2.5 g/cc), which are interpreted as geothermal reservoir areas, indicate that there are 3 (three) geothermal reservoir areas that are separated by fault structures or lithologies (remnants of magmatic processes that was frozen under the peak of Mount Rajabasa.

The high density (2.6 g/cc – 2.7 g/cc) below the summit of Mount Rajabasa is probably related to the remaining magma that has frozen. It is also supported by the high-temperature and a large number of micro-earthquake epicenters under Mount Rajabasa. Therefore, the heat source of the Rajabasa geothermal system must be under the peak of Mount Rajabasa.

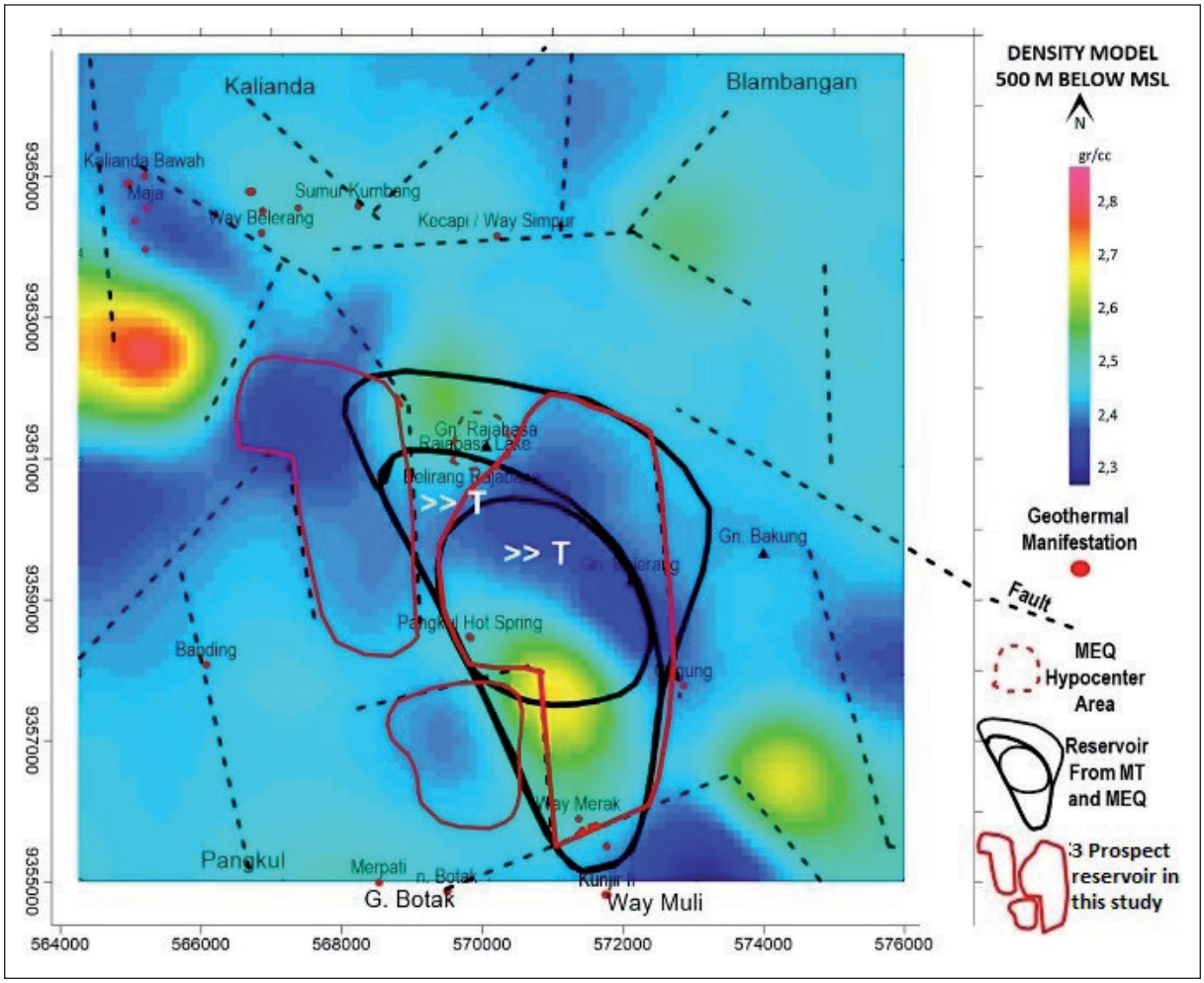

Figure 13. Map of the density distribution model at a depth of 500 m from MSL obtained from the horizontal slice of the inverted 3D density distribution model.

A vertical slice of the inverted 3D density distribution model was performed to obtain a vertical cross-sectional model. The selected cross-section was adjusted to the cross-section of both MT models, so that the density model and the resistivity model from the MT can be compared. Figure 14a shows a cross-sectional model of the residual Bouguer anomaly, a density distribution model (Figure 14b), and a sectional model of the subsurface from MT data for the NW-SE direction (Figure 14c). The 2D profile model shows two geothermal reservoirs in the south (Pangkul-Balirang) and north (north of the peak of Mount Rajabasa), which is in accordance with the MT resistivity cross-sectional model.

The Bouguer anomaly, the SVD anomaly, and the subsurface density distribution model for the west-east path that passes through the Rajabasa Balirang manifestation are shown in Figure 15. This section's analysis and interpretation result indicates two geothermal reservoirs at the east and west of the Balirang Rajabasa manifestation, which is separated by a fault structure.

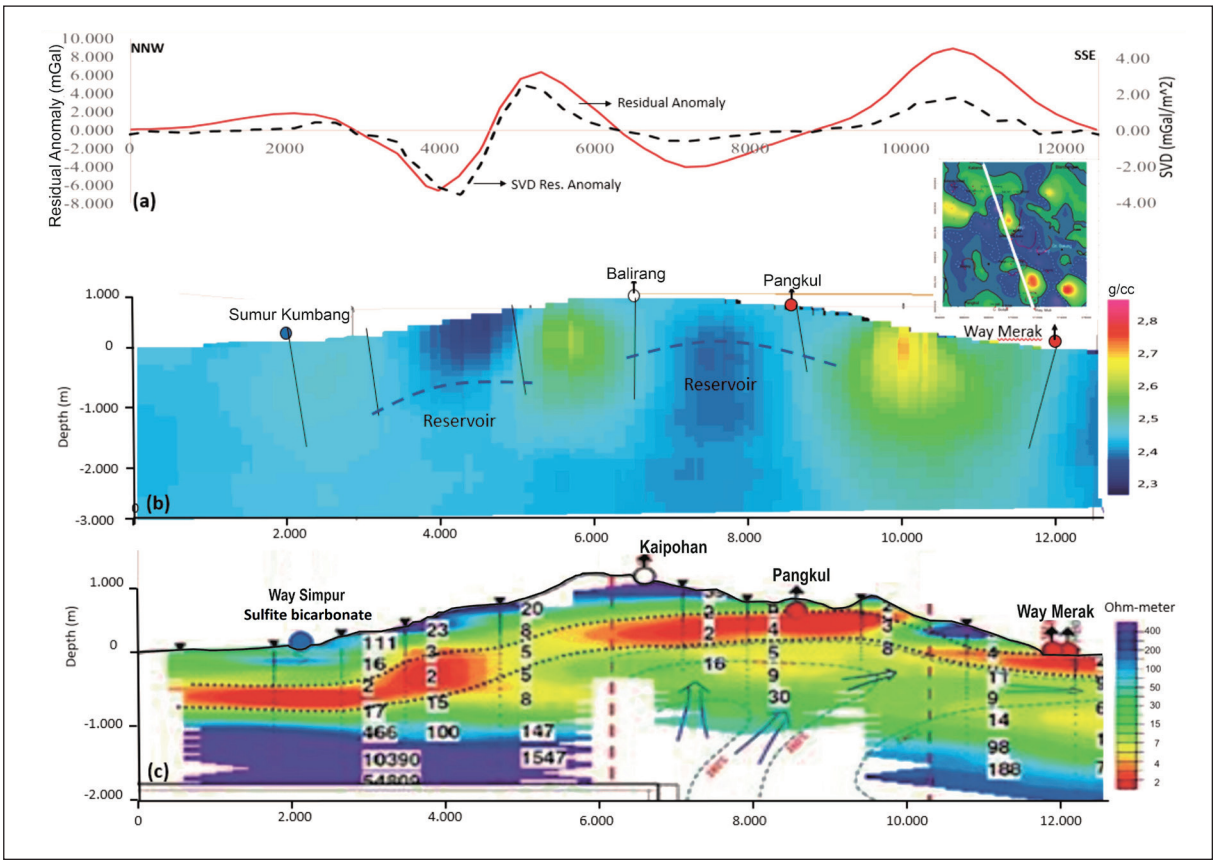

Figure 14. (a) The residual Bouguer anomaly and the SVD from residual Bouguer anomaly, (b) the density distribution of the model inversion, and (c) the resistivity distribution of the MT modeling in NW-SE profiles that crosses geothermal manifestations of Kumbang, Balirang, Pangkul and Way Merak (Saefulhak, 2017).

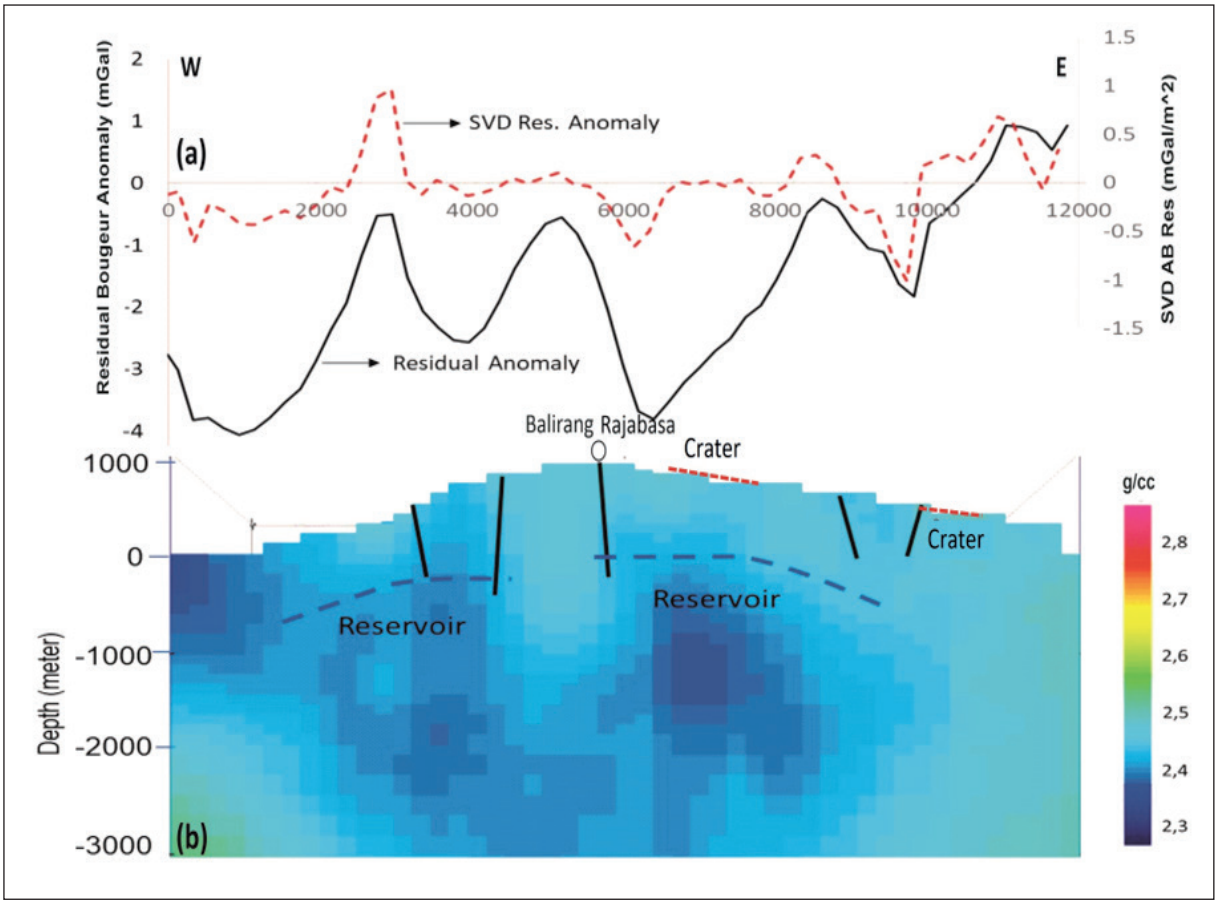

Figure 15. Profile of residual anomaly, SVD, and subsurface density distribution model for the west – east profile that passes through the Rajabasa Balirang manifestation.

CONCLUSION

In Balirang-Rajabasa geothermal region, we completed gravity works, including processing, filtering, and modeling. The results then correlated with geological, geochemical, micro-earthquake, and magnetotelluric data. The Rajabasa geothermal prospect area has a low residual Bouguer anomaly (Δg_{res} <0 mGal), which is correlated with the low-density structure in the area.

Based on the results of the Bouguer residual anomaly, SVD, and the results of the Bouguer Residual anomaly modeling, there are 3 (three) geothermal reservoirs. They are in the area of Mount Balirang, west of Mount Rajabasa, and south of Pangkul hot spring. A fault structure separates the three reservoirs. The properties of the reservoir area, especially the Mount Balirang reservoir, correlate well with MEQ model, temperature, and MT resistivity data.

The heat source from the geothermal system is under Mount Rajabasa, which is indicated by the high density in the area. High density region can be related to the magma path of Mount Rajabasa. The indication is also supported by high temperature data of the area.

The depth of the reservoir in the Rajabasa geothermal prospect area is estimated to be at the depth of 1,000-1,500 m from the ground surface.

ACKNOWLEDGEMENT

The author would like to thank those who have assisted in this work, especially the Geological Survey of Indonesia and the Faculty of Engineering, University of Lampung.

REFERENCES

Abdelrahman, E.M., 1996. Shape and depth solutions from moving average residual gravity anomalies. J. Appl. Geophys. 36, 89–95.

Björbsson, G., Bodvarsson, G., 1990. A survey of geothermal reservoir properties. Geothermics 19, 17–27. https://doi.org/10.1016/0375-6505(90)90063-H

Blakely, R.J., 1995. Potential Theory in Gravity and Magnetic Applications, Program. Cambridge University Press. https://doi.org/10.1017/CBO9780511549816

Brehme, M., Deon, F., Haase, C., Wiegand, B., Kamah, Y., Sauter, M., Regenspurg, S., 2016. Durch Störungszonen kontrollierte geochemische Eigenschaften des geothermischen Reservoirs Lahendong in Indonesien. Grundwasser 21, 29–41. https://doi.org/10.1007/s00767-015-0313-9

Bronto, S., Asmoro, P., Hartono, G., Sulistiyono, 2012. Evolution of Rajabasa Volcano in Kalianda Area and Its Vicinity , South Lampung Regency Evolusi Gunung Api Rajabasa di daerah Kalianda dan Sekitarnya , Kabupaten Lampung Selatan. Indones. J. Geosci. 7, 11–25.

Buyung, N., Walker, A.S.D., 1991. Laporan Penyelidikan Geofisika Gunung Rajabasa.

Daruwati, I.K.A., 2014. Fault Modelling Based on Local Magnetic Anomaly Data in Geothermal Prospect Area Rajabasa Lampung, in: Proceedings of The 4th Annual International Conference Syiah Kuala University (AIC Unsyiah) 2014. Banda Aceh, pp. 72–78.

Elkins, T.A., 1951. The second derivative method of gravity interpretation. Geophysics 16, 29–50. https://doi.org/10.1190/1.1437648

Haerudin, N., Pardede, V.J., Rasimeng, S., Fisika, J., Universitas, F., 2009. Analisis Reservoar Daerah Potensi Panasbumi Gunung Rajabasa Kalianda dengan Metode Tahanan Jenis dan Geotermometer. J. Ilmu Dasar 10, 141–146.

Haerudin, N., Suryanto, W., Sarkowi, M., Risdianto, D., 2014. Magnetic And Gravity Modeling To Determine Reservoir Depth And Prospect Area At Rajabasa Lampung, in: International Conference on Mathematics, Science, and Education 2014 (ICMSE 2014). Semarang.

Haerudin, N., Wahyudi, Suryanto, W., Sarkowi, M., 2013. Analysis of The 3D Geothermal Reservoir Model from Anomaly Magnetic Data Using Mag3D, in: The Third Basic Science International Conference. pp. 1–5.

Harvey, C., 2014. Best Practices Guide For Geothermal Exploration. Bochum.

Hasibuan, R.F., Ohba, T., Abdurrachman, M., Hoshide, T., 2020. Temporal variations of petrological characteristics of Tangkil and Rajabasa volcanic rocks, Indonesia. Indones. J. Geosci. 7, 135–159. https://doi.org/10.17014/ijog.7.2.135-159

Jones, F., 2006. A Program Library for Forward Modelling and Inversion of Gravity Data over 3D Structures. Vancouver.

Mangga, S.A., Amirudin, Suwarti, T., Gafoer, S., Sidarta, 1993. Peta Geologi Lembar Tanjungkarang, Sumatera, skala 1:250.000.

Mussofan, W., Powell, T., Sutrisno, L., Sihotang, M. a, 2015. Geochemistry Model of Chloride Springs Origin near Sea Coastal Area : Case Study from Rajabasa Geothermal Field. World Geotherm. Congr. 2015 19–25.

Mussofan, W., Sutrisno, L., Ramadhan, I., Aulia, N., 2016. Geological Aspects to Constrain Geothermal Conceptual Model : Gunung Rajabasa Case Study, in: Proceedings The 4th Indonesia International Geothermal Convention & Exhibition 2016. Jakarta.

Rasimeng, S., 2008. Daerah Prospek Geothermal Berdasarkan Data Anomali Medan. J. Sains MIPA 14, 67–72.

Saefulhak, Y., 2017. Potensi Panas Bumi Indonesia Jilid 1, Direktorat Panas Bumi, Ditjen EBTKE.

Sarkowi, M., Wibowo, R.C., 2021. Reservoir Identification of Bac-Man Geothermal Field Based on Gravity Anomaly Analysis and Modeling. J. Appl. Sci. Eng. 25, 329–338. http://dx.doi.org/10.6180/jase.202204_25(2).0009.

Setiadi, I., Styanta, B., Widijono, B.S., 2010. Delineasi cekungan sedimen sumatra selatan berdasarkan analisis data gaya berat. J. Geol. dan Sumber Daya Miner. 20, 93–106.

Sumintadireja, P., Dahrin, D., Grandis, H., 2018. A Note on the Use of the Second Vertical Derivative (SVD) of Gravity Data with Reference to Indonesian Cases. J. Eng. Technol. Sci. 50, 127–139. https://doi.org/10.5614/j.eng.technol.sci.2018.50.1.9

Suswati, Haerani, N., Sutawidjaja, I., 2001. Laporan Pemetaan Geologi Gunung Api Rajabasa, Lampung. Bandung.

Witter, J.B., Siler, D.L., Faulds, J.E., Hinz, N.H., 2016. 3D geophysical inversion modeling of gravity data to test the 3D geologic model of the Bradys geothermal area, Nevada, USA. Geotherm. Energy 4. https://doi.org/10.1186/s40517-016-0056-6